# Controlling the Competition between Optically Induced Ultrafast Spin-Flip Scattering and Spin Transport in Magnetic Multilayers

Emrah Turgut,[1] Chan La-o-vorakiat,[1] Justin M. Shaw,[2] Patrik Grychtol,[1] Hans T. Nembach,[2] Dennis Rudolf,[3]
Roman Adam,[3] Martin Aeschlimann,[4] Claus M. Schneider,[3] Thomas J. Silva,[2] Margaret M. Murnane,[1]
Henry C. Kapteyn,[1] and Stefan Mathias[1,4]

[1]*Department of Physics and JILA, University of Colorado, Boulder and NIST, Colorado 80309, USA*
[2]*Electromagnetics Division, National Institute of Standards and Technology, Boulder, Colorado 80305, USA*
[3]*Peter Grünberg Institut, PGI-6 and JARA-FIT, Research Centre Jülich, 52425 Jülich, Germany*
[4]*University of Kaiserslautern and Research Centre OPTIMAS, 67663 Kaiserslautern, Germany*
(Received 20 November 2012; published 7 May 2013)

The study of ultrafast dynamics in magnetic materials provides rich opportunities for greater fundamental understanding of correlated phenomena in solid-state matter, because many of the basic microscopic mechanisms involved are as-yet unclear and are still being uncovered. Recently, two different possible mechanisms have been proposed to explain ultrafast laser induced magnetization dynamics: spin currents and spin-flip scattering. In this work, we use multilayers of Fe and Ni with different metals and insulators as the spacer material to conclusively show that spin currents can have a significant contribution to optically induced magnetization dynamics, in addition to spin-flip scattering processes. Moreover, we can control the competition between these two processes, and in some cases completely suppress interlayer spin currents as a sample undergoes rapid demagnetization. Finally, by reversing the order of the Fe/Ni layers, we experimentally show that spin currents are directional in our samples, predominantly flowing from the top to the bottom layer.

Magnetism, magnetic materials, and studies of dynamics in magnetic materials are all currently areas of great interest, both for the promise of furthering our understanding of correlated matter, and because they are relevant to current and future information technologies, such as data storage and spintronics [1,2]. Dynamic processes in magnetic systems span a broad range of time scales—from domain-wall nucleation and propagation on millisecond to nanosecond time scales [3], to vortex-core flipping and precessional switching on picosecond time scales [4,5], to ultrafast demagnetization [6], spin transport and all-optical switching on femtosecond time scales [7–11]. However, it is difficult to probe the interplay of charge and spin dynamics on both ultrafast timescales and nanometer dimensions, making it very challenging to understand these processes at a fundamental level. This challenge is even more formidable for complex systems such as alloys and multilayer systems [8,10–16]. As a result, the fundamental microscopic mechanisms driving magnetization dynamics on femtosecond timescales are still strongly debated [17–23], and the ultimate physical limit for the speed of magnetic switching and manipulation has not yet been established [7,17–22,24–30].

Recently, two different mechanisms for ultrafast magnetization dynamics have been proposed to explain how ferromagnetic order responds to femtosecond laser pulses: spin-flip scattering [22,24,25,27–29,31] and ultrafast spin transport [7,8,10,11,32–34]. Both theories have been successfully compared with experimental data, but

the microscopic mechanisms they represent are very different. In the case, for instance, of superdiffusive spin transport [7,32], energy-and spin-dependent lifetimes of optically excited hot electrons that are transitional between the ballistic ($x = vt$, where $x$ is the path, $v$ is the velocity of the electron and $t$ is the time) and diffusive ($x = \sqrt{Dt}$, where $D$ is the diffusion constant of the electron) limits [35,36] result in giant spin currents within the material system, which in turn induce femtosecond magnetization dynamics [7,8,10,11,32–34]. Recent theoretical work has proposed that superdiffusive spin transport alone may explain the response of magnetic materials to ultrafast optical excitations [7,32], and recent experimental work seemed to confirm this prediction [37]. In the case of spin-flip scattering, there has been intense debate for more than a decade as to which spin-flip processes (electron-electron, electron-phonon, electron-magnon, direct spin-photon interaction) are relevant to (or dominate) the optically induced magnetization dynamics in various materials [18,20,22,24–29,31,38]. However, to the best of our knowledge, a complete theory that integrates both spin-transport and spin-flip scattering does not yet exist. Given the lack of a complete theory, two important questions need to be addressed experimentally: first, do ultrafast spin-currents contribute significantly in general to ultrafast magnetic processes, beyond the very specific materials systems investigated in Refs. [8,10,28,37]. Second, if so, do spin currents really dominate all ultrafast magnetic processes, as proposed theoretically in Refs. [7,32] and

claimed in the recent experimental work of Eschenlohr *et al.* [37]? Note that such a conclusion would contradict extensive research on spin-flip scattering over the last two decades.

Ultrafast x-ray and extreme-ultraviolet (XUV) sources make it possible to probe element-specific spin dynamics in multispecies magnetic systems [13,39,40]. These nascent optical tools provide new and detailed information not accessible by using visible light, and allow for the design of experiments that can distinguish between different theories of ultrafast spin dynamics. Using tabletop, laser-based, high-harmonic generation (HHG) sources, the fastest spin dynamics in magnetic materials can be simultaneously captured at multiple atomic sites with elemental specificity [40,41]. This powerful new capability allows us to uncover fundamentally new spin dynamics, such as the observation of a 10 to 70 fs delay in the demagnetization of one atomic sublattice with respect to the other in strongly coupled ferromagnetic alloys, as a result of the finite magnitude of quantum-mechanical exchange [14]. More recently, we showed that laser-driven ultrafast, giant, superdiffusive spin-currents can enhance the moment of a buried ferromagnetic layer in magnetic multilayers [8].

In this work, we show that we can control the competition between spin-flip scattering and superdiffusive spin transport in multilayers of Fe/$X$/Ni, where $X$ is a spacer consisting of several different metallic and insulating materials. In particular, by using an insulating spacing layer and an XUV probe that penetrates the entire multilayer sample, we demonstrate complete suppression of interlayer spin-current effects during rapid demagnetization. Our measurements conclusively show that ultrafast spin currents contribute significantly to ultrafast magnetization processes, in addition to the well established and intensively studied spin-flip scattering processes. Finally, by reversing the order of the Fe and Ni layers, we show that ultrafast spin currents are directional, flowing predominantly from the top to the bottom layer of our samples. Thus, spin-flip demagnetization and ultrafast spin-current generation simultaneously contribute to laser-driven femtosecond magnetization dynamics. Our Letter experimentally proves that while spin currents do contribute to ultrafast demagnetization, they alone do not always dominate ultrafast demagnetization as claimed in prior studies [7,32,37]. Moreover, their respective contributions can be controlled by proper sample design.

In our experiment, we use a femtosecond laser pulse to rapidly excite electrons in an Fe/$X$/Ni magnetic multilayer. Coherent HHG light in the XUV is then used in the transverse magneto-optic Kerr effect (T-MOKE) geometry to probe the element-selective magnetic state by measuring the magnetization dependence of the $M_{2,3}$-shell reflectivity for the $3d$ transition metals Fe ($\approx 53$ eV) and Ni ($\approx 67$ eV). HHG pulses ($< 5$ fs) are produced by

focusing an intense laser pulse (25 fs, 2 mJ, 780 nm) into a hollow waveguide filled with Ne [42,43]. The generated HHG spectrum extends from 25 to 72 eV, a range that includes the $M_{2,3}$ absorption edges of both Fe and Ni. In the T-MOKE geometry, the magnetic asymmetry parameter ($A$) is defined as the normalized difference in the reflected intensity ($I_\pm$) of the XUV light upon reversing the magnetization along the axis perpendicular to the plane of incidence: $A = \frac{I_+ - I_-}{I_+ + I_-}$. In the lowest approximation, $A$ is linearly proportional to the magnetization [40,44]. Since the pump and probe beams originate from the same laser pulse, our measurements are intrinsically free of optical jitter. Additional experimental details can be found in Ref. [40].

The multilayer samples consist of substrate/ Ta(3 nm)/Fe(4 nm)/$X$/Ni(5 nm)/Si$_3$N$_4$, where $X$ is the spacer layer. The Si$_3$N$_4$ is used as a capping layer to prevent oxidation of the top layer. The spacer layer $X$ is either a spin transmitter (Ru), a spin scatterer (Ta or W), or an insulator (Si$_3$N$_4$) [45,46]. Samples are fabricated on a SiO$_2$ substrate by dc magnetron sputter deposition. The Ta adhesion layer promotes a uniform texture of the multilayers. The Si$_3$N$_4$ diffraction grating ($\approx 12$ nm) is lithographically patterned on top of the multilayers in order to spectrally disperse the XUV harmonics, which are focused by a toroidal mirror onto a charge-coupled device (CCD) camera. The element-specific T-MOKE signals of both Fe and Ni were simultaneously detected and are clearly distinguished (Fig. 1) allowing for layer-selective investigation of multilayer stacks in the XUV [47]. We switch the magnetic orientations of the magnetic layers with an external ±40 mT field, sufficient to saturate both Ni and Fe (see Supplemental Material [48], Fig. S1).

When optically pumped, the observed magnetization dynamics depend critically on the spacer layer. With 1.7 nm of Ru, there is an abrupt reduction of 68 ± 1% in the Ni asymmetry [Fig. 2(a)]. Such demagnetization is typical of optically excited magnetic systems, as has been extensively studied for two decades. In contrast, the Fe asymmetry *increases* by 16 ± 1%, indicative of a magnetization enhancement (See the Supplemental Material [48]). This new observation of an optically pumped magnetization enhancement was recently reported by us, and explained as arising due to superdiffusive spin transport between the Ni and Fe layers [8]. The femtosecond pump pulse generates a nonequilibrium, hot electron distribution in the magnetic layers. Energy- and spin-dependent hot-electron lifetimes modulate the electron distribution, giving rise to a spin current [49,50] that flows preferentially from Ni to Fe. The spin-current is initially ballistic on time scales of 5 to 10 fs, after which it becomes diffusive as the electrons thermalize [7,32], hence, the superdiffusive character of the spin current.

To experimentally explore the contributions of spin-flip scattering and spin-transport processes to optically induced
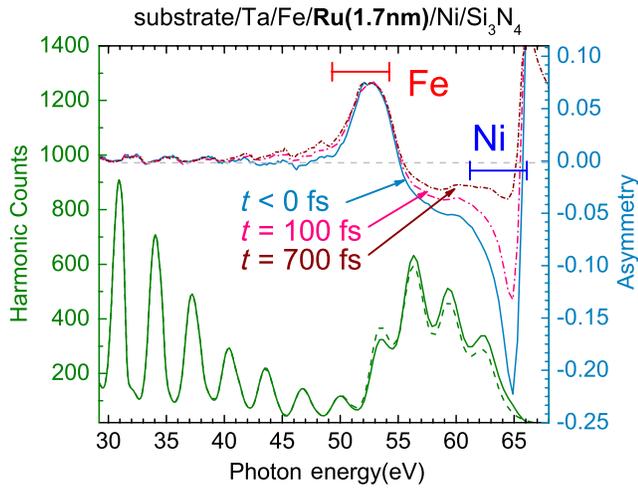
FIG. 1 (color online). Temporal evolution of the magnetic asymmetry and the reflected XUV spectrum of a substrate/ Ta(3 nm)/Fe(4 nm)/Ru(1.7 nm)/Ni(5 nm)/Si$_3$N$_4$(6 nm) multilayer. The solid and dashed green curves represent the reflected XUV intensities upon reversal of the external magnetic field. The light blue curve denotes the derived static (no pump) magnetic asymmetry, which is maximum at the $M_{2,3}$ absorption edges of Fe (red bar) and Ni (blue bar) and linearly proportional to the magnetization. The pink and the brown curves show the magnetic asymmetry after excitation by a laser pump pulse at a pump-probe delay of $+100$ and $+700$ fs, respectively. Figure 2(a) is obtained by integrating over the Fe (red bar) and Ni (blue bar) regions of the asymmetry curve.

demagnetization, we fabricated multilayer samples with Ta and W spacers, which have spin diffusion lengths ($\mathcal{L}_s$) of only a few nanometers [45,46] (in contrast to $\mathcal{L}_s = 14$ nm for Ru [51]). Then, to strongly suppress the contribution of spin diffusion to the dynamic magnetic response, we used an insulating spacer of Si$_3$N$_4$. (We note that reported values for $\mathcal{L}_s$ are measured at the Fermi energy $E_F$. While it is not yet known how the $\mathcal{L}_s$ depends on energy above $E_F$, we expect a weak dependence of $\mathcal{L}_s$ on energy under the assumption that spin flip is due to Elliot-Yafet scattering from defects with large spin-orbit coupling.) These samples with different spacer materials permit us to distinguish between the ultrafast spin-transport and spin-flip scattering mechanisms; we expect a weaker or absent enhancement of the Fe magnetization when a spin scatterer or insulator is placed between the Ni and Fe layers.

Figures 2(b)–2(d) show the measurement results for these samples in the case of parallel Ni and Fe magnetizations and nearly identical pump fluences (for high-fluence data see Ref. [8]). For all three samples, the magnetization of Ni decreases by $\approx 50\%$ at similar rates, while the magnetization of the Fe layer decreases by $13 \pm 1\%$ and $5 \pm 1\%$ for 2 nm Ta and W, respectively, and $23 \pm 1\%$ for 3 nm Si$_3$N$_4$. Note that the large Fe demagnetization in the case of a Si$_3$N$_4$ spacer is not strictly the result of obstructed spin-current flow between Ni and
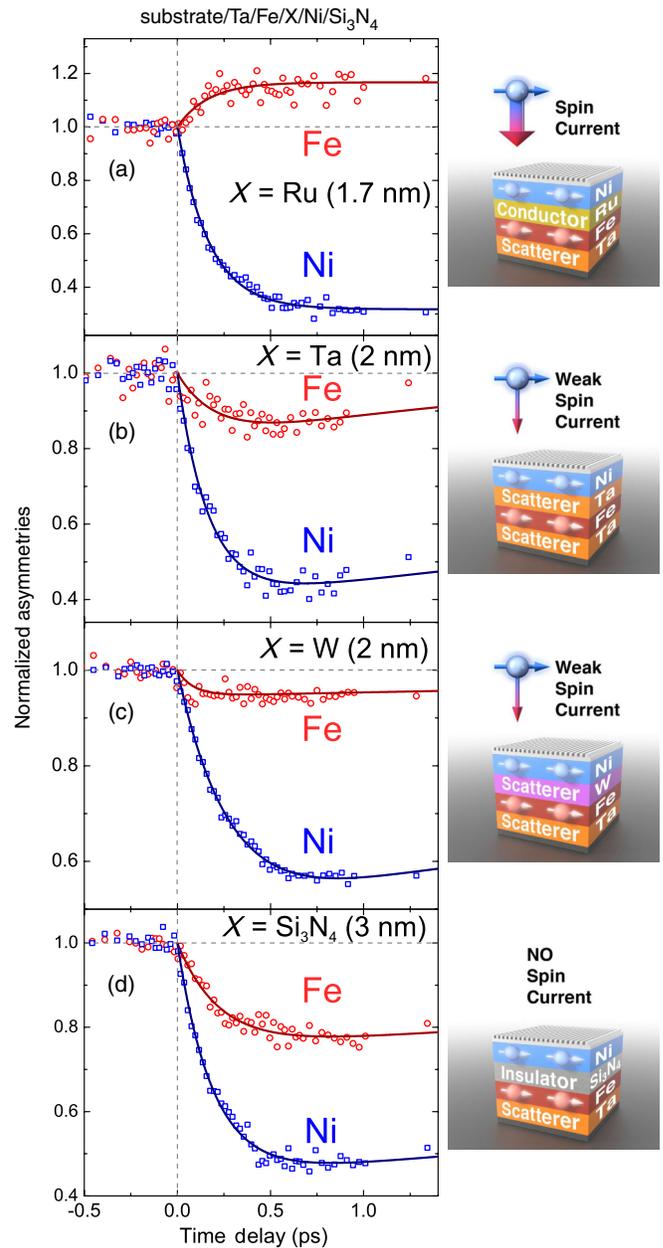


FIG. 2 (color online). Layer-selective magnetization dynamics in substrate/Ta(3 nm)/Fe(4 nm)/$X$/Ni(5 nm)/Si$_3$N$_4$(6 nm) multilayers with different spacer layers. In (a), clear enhancement in the magnetization of the Fe layer is observed in the presence of good spin transport across the 1.7 nm Ru spacer layer. In (b) and (c), no enhancement of the magnetization of the Fe layer is observed when spin scattering spacer layers of Ta (2 nm) and W (2 nm) are used. In (d), spin currents are fully suppressed by inserting a 3 nm insulating Si$_3$N$_4$ layer.

Fe; spin-flip demagnetization of Fe is larger because Si$_3$N$_4$ is more transparent. Indeed, optical matrix calculations show that the absorbance of the Fe layer is 15% larger for the Si$_3$N$_4$ spacer. (See the Supplemental Material [48]).

Comparison of the data for samples with different spacer layer materials indicates that interlayer spin-current

propagation is not the only operative mechanism for ultra-fast demagnetization. By using materials with a short spin lifetime as the spacer, spin transport between Ni and Fe should be reduced or even eliminated; however, we find that both the Ni and the Fe layers still demagnetize. We empha-size that our technique is sensitive to the average magneti-zation within a given layer, not the gradient of the spin accumulation that might result from intralayer spin cur-rents, in contrast to what was suggested in Ref. [32] in regard to T-MOKE experiments with optically thick mag-netic layers. Given that we observe demagnetization in both the top Ni layer and buried Fe layer, we confirm that spin-flip scattering must necessarily contribute to the dynamics. This is in contrast to recent theoretical and experimental works on superdiffusive spin currents, [7,32,37], which claim spin transport as the only relevant process, and are not in accordance with two decades of experimental and theoretical work on spin-flip scattering in femtomagnetism. Note that although spin-transport and spin-flip scattering represent two very different microscopic interactions, their induced magnetization dynamics clearly evolve on identi-cal time scales [see Figs. 2(a) and 2(d)]. This is why it was so challenging until now to disentangle their contributions using other measurement techniques.

In all of the sample systems considered so far, there is a preferential flow of majority spins from Ni to Fe. This has been explained in terms of the large spin transport asym-metry of hot electrons for Ni in comparison to Fe (Ref. [8] and Supplemental Material [48]). If this were indeed the case, the inversion of Ni and Fe in the multilayer stack should still result in majority spin-current flow from Ni to Fe, given that the optical absorbance of the Ni and Fe layers is only weakly dependent on their order in the stack. (See Supplemental Material [48], Table S1.) Thus, we would expect that the magnetization change in Fe would still show a strong dependence on the relative orientation of the magnetization in the two layers. Surprisingly, however, when we repeated our measurements for a sample where Fe is on top [substrate/Ta(3 nm)/Ni(5 nm)/Ru(1.7 nm)/Fe(4 nm)/Si$_3$N$_4$(6 nm)] only the Ni layer shows any sig-nificant dependence of the demagnetization amplitude on the relative orientation, as shown in Fig. 3. The demagne-tization of Ni is $38 \pm 1\%$ and $56 \pm 4\%$ for parallel and antiparallel alignments, respectively, while the magnetiza-tion of Fe is only slightly affected by the relative orienta-tion. We infer from the data that the Fe majority spins are now flowing from Fe to Ni, despite the fact that the optical absorbance of the two ultrathin layers is virtually unchanged. One plausible explanation for the apparent inversion of spin-current flow direction is that the Ta seed layer acts as a strong spin scatterer, substantially reducing the majority spin current emitted by the buried layer, whether it be Ni or Fe. The spin current from the top layer will be stronger in the downward direction into the multilayer due to the presence of the surface, while the spin
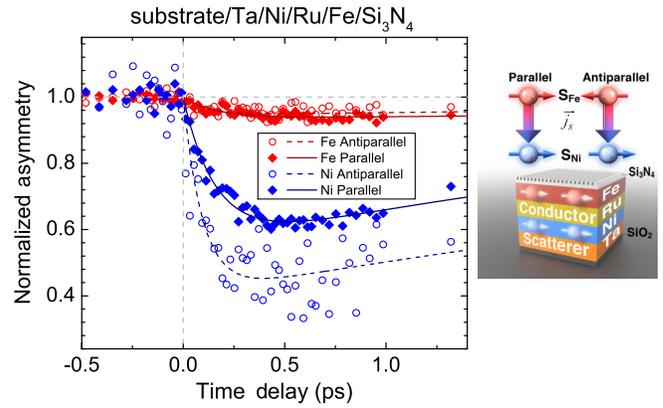


FIG. 3 (color online).   Magnetization dynamics of a substrate/Ta(3 nm)/Ni(5 nm)/Ru(1.7 nm)/Fe(4 nm)/Si$_3$N$_4$(6 nm) mul-tilayer. Parallel and antiparallel alignments of the Ni and Fe layers are, respectively obtained by using a strong ($\pm 40$ mT) and weak ($\pm 10$ mT) external magnetic field (see the Supplemental Material [48]). The observed demagnetization in the Fe layer does not change as a function of the relative magnetic orientation. In contrast, demagnetization in the Ni layer increases from $\approx 38 \pm 1\%$ to $56 \pm 4\%$ for antiparallel orientation, because spin currents from the top (Fe) layer to the bottom (Ni) layer favor spin-flip scattering processes.

current from the bottom layer upwards will be weaker due to scattering of downward-propagating spin current in the Ta seed layer. Another possible explanation might be re-lated to calorimetric processes, induced by the gradient of the laser light absorption within the layers.

The data of Fig. 3 are consistent with a simultaneous occurrence of interlayer spin-current flow and spin-flip demagnetization processes. It is generally known that the optically driven demagnetization of a single Fe layer is weaker than that of Ni under identical pump fluence [14]. We also know that the buried Fe layer absorbs marginally less light than when it is on the top of the stack. In that case, the magnetization change of the buried Fe layer is primar-ily driven by interlayer spin-current transport, and only secondarily by intrinsic spin-flip processes. On the other hand, when Fe is on top, the Fe-majority spin current now flows into the Ni as explained above, but since spin-flip demagnetization processes are much stronger in Ni, the amount of demagnetization in Ni for parallel orientation is reduced. The effect of ultrafast spin currents from the Fe into the Ni is not sufficient to induce an overall magneti-zation enhancement, in contrast to the case when Ni is on the top.

Finally, quantitative accounting of the magnetization change in the Ni and Fe layers can be used to show that both spin-flip processes and intralayer spin currents are simultaneously present. Taking the atomic magnetic moments ($0.65\mu_B$ for Ni and $2.2\mu_B$ for Fe) and atomic concentrations ($9.14 \times 10^{28}$ m$^{-3}$ for Ni and $8.50 \times 10^{28}$ m$^{-3}$ for Fe) into account [52], a lossless transfer of spin between Fe and Ni should result in an approximately

3× larger change in the magnetization of Ni compared to Fe. Thus, a 48% reduction of the Ni magnetization is required to enhance the Fe magnetization by $16 \pm 1\%$, as observed in Fig. 2(a), under the assumption that the spin-current consists primarily of Ni majority spins, and that the magnetization change in Fe is primarily due to interlayer spin currents (as seen before in Ref. [8]). However, the Ni demagnetization in Fig. 2(a) is $68 \pm 1\%$, suggestive that spin-flip processes account for roughly a third of the Ni demagnetization when Ni is the top layer. Similarly, the observed Ni demagnetization in Fig. 3 of $38 \pm 1\%$ and $56 \pm 1\%$ for parallel and antiparallel alignment, respectively, requires a minimum demagnetization of 3% for Fe. Again, this is approximately half as large as the Fe demagnetization shown in Fig. 3, consistent with a hypothesis that half of the Fe demagnetization is the result of intrinsic spin-flip processes. Note that hot spin-polarized electrons that are lost due to ultrafast spin transport into another layer will influence the hot-electron spin-flip scattering rate inside the original layer. It is therefore not straightforward to compare demagnetization amplitudes between the different material systems. First, a theoretical picture including both processes needs to be developed.

In summary, we show that both interlayer spin currents and intrinsic spin-flip processes play an important role in optically driven ultrafast magnetization dynamics for the case of magnetic multilayers, depending critically on the composition of the investigated system. Both phenomena are comparable in magnitude for the samples studied here, and thus, a complete theory for ultrafast magnetization dynamics should include both mechanisms. Moreover, their respective strengths can be controlled by changing the design of the sample, which can also influence the directional flow of spin current.

[1] I. Zutic, J. Fabian, and S. Sarma, Rev. Mod. Phys. **76**, 323 (2004).

[2] C. Chappert, A. Fert, and F. N. Van Dau, Nat. Mater. **6**, 813 (2007).

[3] D. A. Allwood, G. Xiong, C. C. Faulkner, D. Atkinson, D. Petit, and R. P. Cowburn, Science **309**, 1688 (2005).

[4] R. Hertel, S. Gliga, M. Fähnle, and C. M. Schneider, Phys. Rev. Lett. **98**, 117201 (2007).

[5] T. Gerrits, H. A. M. Van Den Berg, J. Hohlfeld, L. Bär, and T. Rasing, Nature (London) **418**, 509 (2002).

[6] E. Beaurepaire, J. C. Merle, A. Daunois, and J. Y. Bigot, Phys. Rev. Lett. **76**, 4250 (1996).

[7] M. Battiato, K. Carva, and P. M. Oppeneer, Phys. Rev. Lett. **105**, 027203 (2010).

[8] D. Rudolf, C. La-O-Vorakiat, M. Battiato, R. Adam, J. M. Shaw, E. Turgut, P. Maldonado, S. Mathias, P. Grychtol, H. T. Nembach, T. J. Silva, M. Aeschlimann, H. C. Kapteyn, M. M. Murnane, C. M. Schneider, and P. M. Oppeneer, Nat. Commun. **3**, 1037 (2012).

[9] A. Kirilyuk, A. Kimel, and T. Rasing, Rev. Mod. Phys. **82**, 2731 (2010).

[10] A. Melnikov, I. Razdolski, T. O. Wehling, E. T. Papaioannou, V. Roddatis, P. Fumagalli, O. Aktsipetrov, A. I. Lichtenstein, and U. Bovensiepen, Phys. Rev. Lett. **107**, 076601 (2011).

[11] G. Malinowski, F. Dalla Longa, J. H. H. Rietjens, P. V. Paluskar, R. Huijink, H. J. M. Swagten, and B. Koopmans, Nat. Phys. **4**, 855 (2008).

[12] G. M. Müller, J. Walowski, M. Djordjevic, G.-X. Miao, A. Gupta, A. V. Ramos, K. Gehrke, V. Moshnyaga, K. Samwer, J. Schmalhorst, A. Thomas, A. Hütten, G. Reiss, J. S. Moodera, and M. Münzenberg, Nat. Mater. **8**, 56 (2009).

[13] I. Radu, K. Vahaplar, C. Stamm, T. Kachel, N. Pontius, H. A. Dürr, T. A. Ostler, J. Barker, R. F. L. Evans, R. W. Chantrell, A. Tsukamoto, A. Itoh, A. Kirilyuk, T. Rasing, and A. V. Kimel, Nature (London) **472**, 205 (2011).

[14] S. Mathias, C. La-O-Vorakiat, P. Grychtol, P. Granitzka, E. Turgut, J. M. Shaw, R. Adam, H. Nembach, M. Siemens, S. Eich, C. M. Schneider, T. J. Silva, M. Aeschlimann, M. M. Murnane, and H. C. Kapteyn, Proc. Natl. Acad. Sci. U. S. A. **109**, 4792 (2012).

[15] D. Steil, S. Alebrand, T. Roth, M. Krauß, T. Kubota, M. Oogane, Y. Ando, H. C. Schneider, M. Aeschlimann, and M. Cinchetti, Phys. Rev. Lett. **105**, 217202 (2010).

[16] S. Mathias *et al.*, J. Electron Spectrosc. Relat. Phenom., doi: 10.1016/j.elspec.2012.11.013 (2012).

[17] G. P. Zhang, W. Hübner, G. Lefkidis, Y. Bai, and T. F. George, Nat. Phys. **5**, 499 (2009).

[18] K. Carva, M. Battiato, and P. Oppeneer, Phys. Rev. Lett. **107**, 207201 (2011).

[19] K. Carva, M. Battiato, and P. M. Oppeneer, Nat. Phys. **7**, 665 (2011).

[20] S. Essert and H. C. Schneider, Phys. Rev. B **84**, 224405 (2011).

[21] B. Y. Mueller, T. Roth, M. Cinchetti, M. Aeschlimann, and B. Rethfeld, New J. Phys. **13**, 123010 (2011).

[22] T. Roth, A. J. Schellekens, S. Alebrand, O. Schmitt, D. Steil, B. Koopmans, M. Cinchetti, and M. Aeschlimann, Phys. Rev. X **2**, 021006 (2012).

[23] C. Stamm, T. Kachel, N. Pontius, R. Mitzner, T. Quast, K. Holldack, S. Khan, C. Lupulescu, E. F. Aziz, M. Wietstruk, H. A. Dürr, and W. Eberhardt, Nat. Mater. **6**, 740 (2007).

[24] E. Carpene, E. Mancini, C. Dallera, M. Brenna, E. Puppin, and S. De Silvestri, Phys. Rev. B **78**, 174422 (2008).

[25] A. B. Schmidt, M. Pickel, M. Donath, P. Buczek, A. Ernst, V. P. Zhukov, P. M. Echenique, L. M. Sandratskii, E. V. Chulkov, and M. Weinelt, Phys. Rev. Lett. **105**, 197401 (2010).

[26] J.-Y. Bigot, M. Vomir, and E. Beaurepaire, Nat. Phys. **5**, 515 (2009).

[27] M. Krauß, T. Roth, S. Alebrand, D. Steil, M. Cinchetti, M. Aeschlimann, and H. Schneider, Phys. Rev. B **80**, 180407 (2009).

[28] B. Koopmans, G. Malinowski, F. Dalla Longa, D. Steiauf, M. Fahnle, T. Roth, M. Cinchetti, and M. Aeschlimann, Nat. Mater. **9**, 259 (2010).

[29] M. Sultan, U. Atxitia, A. Melnikov, O. Chubykalo-Fesenko, and U. Bovensiepen, Phys. Rev. B **85**, 184407 (2012).

[30] U. Atxitia and O. Chubykalo-Fesenko, J. Walowski, A. Mann, and M. Munzenberg, Phys. Rev. B **81**, 174401 (2010).

[31] M. Cinchetti, M. Sánchez Albaneda, D. Hoffmann, T. Roth, J.-P. Wüstenberg, M. Krauß, O. Andreyev, H. C. Schneider, M. Bauer, and M. Aeschlimann, Phys. Rev. Lett. **97**, 177201 (2006).

[32] M. Battiato, K. Carva, and P. M. Oppeneer, Phys. Rev. B **86**, 024404 (2012).

[33] B. Vodungbo, J. Gautier, G. Lambert, A. B. Sardinha, M. Lozano, S. Sebban, M. Ducousso, W. Boutu, K. Li, B. Tudu, M. Tortarolo, R. Hawaldar, R. Delaunay, V. López-Flores, J. Arabski, C. Boeglin, H. Merdji, P. Zeitoun, and J. Lüning, Nat. Commun. **3**, 999 (2012).

[34] B. Pfau, S. Schaffert, L. Müller, C. Gutt, A. Al-Shemmary, F. Büttner, R. Delaunay, S. Düsterer, S. Flewett, R. Frömter, J. Geilhufe, E. Guehrs, C. M. Günther, R. Hawaldar, M. Hille, N. Jaouen, A. Kobs, K. Li, J. Mohanty, H. Redlin, W. F. Schlotter, D. Stickler, R. Treusch, B. Vodungbo, M. Kläui, H. P. Oepen, J. Lüning, G. Grübel, and S. Eisebitt, Nat. Commun. **3**, 1100 (2012).

[35] M. Aeschlimann, M. Bauer, S. Pawlik, W. Weber, R. Burgermeister, D. Oberli, and H. C. Siegmann, Phys. Rev. Lett. **79**, 5158 (1997).

[36] V. P. Zhukov, E. V. Chulkov, and P. M. Echenique, Phys. Rev. B **73**, 125105 (2006).

[37] A. Eschenlohr, M. Battiato, P. Maldonado, N. Pontius, T. Kachel, K. Holldack, R. Mitzner, A. Föhlisch, P. M. Oppeneer, and C. Stamm, Nat. Mater. **12**, 332 (2013).

[38] G. P. Zhang, Y. Bai, W. Hubner, G. Lefkidis, and T. F. George, J. Appl. Phys. **103**, 07B113 (2008).

[39] C. La-O-Vorakiat, M. Siemens, M. M. Murnane, H. C. Kapteyn, S. Mathias, M. Aeschlimann, P. Grychtol, R. Adam, C. M. Schneider, J. M. Shaw, H. Nembach, and T. J. Silva, Phys. Rev. Lett. **103**, 257402 (2009).

[40] C. La-O-Vorakiat, E. Turgut, C. A. Teale, H. C. Kapteyn, M. M. Murnane, S. Mathias, M. Aeschlimann, C. M. Schneider, J. M. Shaw, H. T. Nembach, and T. J. Silva, Phys. Rev. X **2**, 011005 (2012).

[41] J.-Y. Bigot, Physics **5**, 5 (2012).

[42] H. C. Kapteyn, M. M. Murnane, and I. P. Christov, Phys. Today **58**, No. 3, 39 (2005).

[43] T. Popmintchev, M.-C. Chen, P. Arpin, M. M. Murnane, and H. C. Kapteyn, Nat. Photonics **4**, 822 (2010).

[44] P. M. Oppeneer, in *Handbook of Magnetic Materials*, edited by K. H. J. Buschow (Elsevier, Amsterdam, 2001), p. 229.

[45] M. Morota, Y. Niimi, K. Ohnishi, D. H. Wei, T. Tanaka, H. Kontani, T. Kimura, and Y. Otani, Phys. Rev. B **83**, 174405 (2011).

[46] J. Bass and W. P. Pratt, J. Phys. Condens. Matter **19**, 183201 (2007).

[47] P. Grychtol, R. Adam, S. Valencia, S. Cramm, D. E. Bürgler, and C. M. Schneider, Phys. Rev. B **82**, 054433 (2010).

[48] See Supplemental Material at http://link.aps.org/supplemental/10.1103/PhysRevLett.110.197201 for understanding the magnetic switching behavior of the Ni and Fe layers, for more details on the data analysis, for tables of the absorption ratios of the pump beam by all layers as well as demagnetization amounts of the Ni and Fe layers in different samples.

[49] M. Aeschlimann, M. Bauer, S. Pawlik, R. Knorren, G. Bouzerar, and K. H. Bennemann, Appl. Phys. A **71**, 485 (2000).

[50] R. Knorren, G. Bouzerar, and K. H. Bennemann, Phys. Rev. B **63**, 125122 (2001).

[51] K. Eid, R. Fonck, M. A. Darwish, W. P. Pratt, and J. Bass, J. Appl. Phys. **91**, 8102 (2002).

[52] J. Stöhr and H. C. Siegmann, *Magnetism: From Fundamentals to Nanoscale Dynamics* (Springer, New York, 2006).